Induction of growth arrest and apoptosis in human breast cancer cells by 3,3-diindolylmethane is associated with induction and nuclear localization of $p27^{kip}$

Zhiwei Wang,[1] Bennett W. Yu,[2] KM Wahidur Rahman,[1] Fakhara Ahmad,[1] and Fazlul H. Sarkar[1]

[1]Department of Pathology, Karmanos Cancer Institute, Wayne State University School of Medicine, Detroit, Michigan and [2]Medical Oncology, Peninsula Regional Medical Center, Salisbury, Maryland

Abstract

3,3′-Diindolylmethane (DIM) is a stable condensation product of indole-3-carbanol, a potential breast cancer chemoprevention agent. Human breast cancer cell lines were studied to better understand its mechanisms. *In vitro* experiments were done in MCF-7, T47D, BT-20 and BT-474 cells using MTT, ELISA, immunoblotting assays, reverse transcription-PCR, protein half-life, confocal microscopy, cell fractionation, and immunoprecipitation assays. We found that DIM inhibited the growth of all four breast cancer cell lines (IC_{50}s, 25-56 μmol/L). Because BT-20 and BT-474 overexpressed Her-2 and activated Akt, and BT-20 lacks estrogen receptor, these were studied further. In both cell lines, DIM appeared to induce expression of $p27^{kip}$ protein before the loss of cell viability and apoptosis. In BT-20 cells, DIM also inhibited expression of activated Akt, but this appeared after $p27^{kip}$ induction. In both cell lines, DIM induced $p27^{kip}$ transcript expression within 6 h. DIM prolonged the $p27^{kip}$ protein half-life in BT-20 but not BT-474 cells. We also showed, for the first time, that DIM induced nuclear localization of $p27^{kip}$ in both cell lines. Moreover, in BT-20 cells, DIM induced a decrease in $p27^{kip}$ phosphorylation at Thr^{187}, and its association with the 14-3-3 protein, which helped to explain the protein half-life increase and nuclear localization, respectively. DIM modulates $p27^{kip}$ through transcription, prolongation of protein half-life, and nuclear localization. These effects appear to be independent of Her-2, Akt, or estrogen receptor status and should support further study for its chemoprevention potential in breast cancer. [Mol Cancer Ther 2008;7(2):341–9]

Introduction

Breast cancer remains the second most common and lethal malignancy in women worldwide. The accepted prevention agent in breast cancer is tamoxifen, which is limited to a ~45% reduction in the risk of breast cancer (1). Because its mechanism of action is dependent on the presence of the estrogen receptor (ER), it does not appear to influence treatment of cancers that are ER negative. Other hormonal agents under clinical investigation (e.g., aromatase inhibitors) will likely be limited in their efficacy in preventing ER-negative tumors, because their mechanism of action is the inhibition of peripheral conversion of estrogen. In advanced metastatic breast cancer, response duration and survival prolongation are measured in months despite many available chemotherapies (2). Newer hormonal agents, such as aromatase inhibitors, yield only a 15% to 20% response rate with major cross-resistance with tamoxifen (3). Thus, there is a clear need to develop other prevention or treatment approaches with low side effect profiles.

Epidemiologic data suggest that, in Asian regions, diets rich in cruciferous vegetables are associated with a markedly reduced incidence of breast cancer (4). Studies have shown that cruciferous vegetables, particularly cabbage, broccoli, and Brussels sprouts, are a rich source of many phytochemicals, including indole derivatives, such as indole-3-carbanol (I3C). I3C is an effective oral chemopreventive agent that can inhibit mammary tumors in carcinogen-induced rat models and in a v-H-ras transgenic mouse model (5, 6). I3C, in a low pH environment, is easily converted to its dimeric product 3,3′-diindolylmethane (DIM). DIM may be responsible for many of the biological effects attributed to I3C. For example, in a sensitive trout hepatocarcinogenesis model, DIM, but not I3C, was chemopreventive when both molecules were administered by injection (7). DIM also markedly prevented further growth of established (100-200 mm^3) 7,12-dimethylbenz[*a*]anthracene-induced breast tumors in rats (8). Because of the potential application of DIM in breast cancer prevention, we sought to better understand its mechanisms of action.

DIM not only inhibits cell growth and DNA synthesis but also induces apoptosis in MCF-7 and T47D ER-positive breast cancer cells (8, 9). Inhibition of DNA synthesis and

Received 7/16/07; revised 11/16/07; accepted 12/28/07.

The costs of publication of this article were defrayed in part by the payment of page charges. This article must therefore be hereby marked *advertisement* in accordance with 18 U.S.C. Section 1734 solely to indicate this fact.

Note: Z. Wang and B.W. Yu equally contributed to this work.

Requests for reprints: Fazlul H. Sarkar, Department of Pathology, Karmanos Cancer Institute, Wayne State University School of Medicine, 9374 Scott Hall, 540 East Canfield, Detroit, MI 48201.
Phone: 313-576-8327; Fax: 313-576-8389;
E-mail: sarkarf@karmanos.org

doi:10.1158/1535-7163.MCT-07-0476

induction of apoptosis in ER-negative MDA-MB-231 breast cancer cells by DIM has also been shown (10). However, the mechanisms of these effects are only partly understood. Although I3C has been shown to induce p21 and p27 in breast cancer cells (11), this has not been confirmed for DIM. Recently, we have reported that DIM can inhibit Akt activation in MCF10A breast cancer cells (12). Akt is a reasonable molecular target in breast cancer as it is activated in the majority of breast cancer cell lines and tumors (13).

Based on the above information, we hypothesized that the blockade of Akt signaling and induction of $p27^{kip}$ by DIM are linked events, because Akt can phosphorylate and repress the forkhead family of transcription factors (14), which are known to transactivate the $p27^{kip}$ promoter (15). Moreover, it has been recently reported that Akt is one of several kinases that can directly phosphorylate $p27^{kip}$ at multiple sites, resulting in the nuclear export of $p27^{kip}$ (16), its cytoplasmic localization through 14-3-3 binding (17), or its degradation by the ubiquitin-ligase proteozyme complex (18). In this report, we examined if DIM could reciprocally inhibit Akt and induce $p27^{kip}$ and thus explored potential mechanisms. BT-20 and BT-474 breast cancer cells were selected for further study because of the limited information on the effect of DIM on breast cancer cells, particularly those with overexpression of Her-2 or activated Akt.

Materials and Methods

Cell Lines and Culture Methods

MCF-7, T47D, BT-20, and BT-474 cells were obtained from American Type Culture Collection and cultured according to recommended conditions. For all experiments, cells were used with 20 or fewer passages after being received from American Type Culture Collection. MCF-7 cells were cultured in DMEM, whereas the others were cultured in RPMI. All media were supplemented with 10% FCS, 2 mmol/L glutamine, 100 units/mL penicillin, and 100 μg/mL streptomycin (all culture reagents from Invitrogen).

Reagents

DIM (LKT) from one stock was used for all experiments, diluted in DMSO at 100 mmol/L stocks frozen at −80°C for up to 6 months, conditions that maintained stability for up to 6 months according to the supplier.

MTT Growth Assay

Growth inhibition by DIM was determined by a MTT assay. Subconfluent cells were trypsinized and plated in 96-well culture plates at 5,000 cells in 200 μL complete medium added to a quadruplet set of wells for each DIM concentration. The next day (day 0), complete medium was changed with DIM at the desired final concentrations. A baseline plate was assayed on day 0. After 5 days of incubation, cell mass was measured by adding 40 μL MTT at 5 mg/mL (Sigma) per well followed by incubation at 37°C for 2 h. Wells were aspirated, 100 μL isopropanol was added, and plates were gently shaken for 30 min. Absorption at 595 nm was measured on an Ultra plate reader (Tecan). After the background signal of medium-containing blank wells was subtracted from all wells, values were normalized to the day 0 average values, and the relative growth inhibition by DIM wells was calculated by dividing the values from control wells without DIM. Relative growth mean and SD was graphed versus log DIM concentration, and IC_{50} was calculated by a sigmoidal dose-response curve with Prism software (GraphPad). The IC_{50} values presented are the average of at least two independent experiments.

Apoptosis Assay

Nucleosomal DNA was assayed with the ELISA^{PLUS} (Roche) kit using the provided protocol with minor modifications. BT-20 or BT-474 cells were plated in duplicate wells at 2.0×10^5 per well in six-well dishes and cultured overnight. DIM was added at 0 and 50 μmol/L (BT-474) or 100 μmol/L (BT-20). At 24, 48, and 72 h, both floating and trypsinized cells were collected and washed and both viable and dead cells were counted by trypan staining. Fifty-thousand cells (live or dead) were extracted with 500 μL incubation buffer, and after pelleting, the supernatant was saved at −20°C. A sample of 100 μL of each extract (diluted 1:10 in incubation buffer) was processed per protocol. Signal was assayed for absorption at 405 nm in the Ultra plate reader. The mean and SD from at least two independent experiments (n of at least 4) were plotted with Prism software.

Immunoblotting

Cells were cultured at 5×10^6 in 150-mm dishes to 50% to 60% confluence. Total cell extract was prepared from scraped cells as described previously (19) with minor modifications. The lysis buffer included 1 mmol/L phenylmethylsulfonyl fluoride, 1 μg/mL pepstatin, and 4% (v/v) protease inhibitor cocktail (Roche). Protein concentration was measured with the BCA kit (Pierce) and 50 μg were electrophoresed in 10% to 16% denaturing acrylamide gels and transferred to Optiran reinforced nitrocellulose membranes (Schleicher & Schuell). Membranes were blocked in PBS with 5% milk and 0.1% Tween 20 followed by incubation with primary antibodies in blocking buffer (or in PBS with 5% bovine serum albumin and 0.1% Tween 20 for anti-phospho-substrate antibodies) overnight at 4°C. Primary antibodies were anti-Her-2 at 1:40 (OP-15; Calbiochem), anti-Akt1 at 1:1,000 (9272; Cell Signaling), anti-phospho-Akt at 1:1000 (9271; Cell Signaling), anti-$p27^{kip}$ at 1:1,000 (sc-528; Santa Cruz), and anti-actin at 1:5,000 (A5441; Sigma). Appropriate secondary horseradish peroxidase–linked antibodies (Amersham or Bio-Rad) were used. Membranes were developed with SuperSignal chemiluminescence (Pierce) and images captured on film, scanned as Adobe files, and formatted in PowerPoint. Densitometry was done on a Gel Doc 1000 (Bio-Rad), and signals were normalized to actin expression and displayed in bar graphs. Values from at least three different gels from two or more independent experiments were included in the analysis.

For testing effects of DIM on protein expression, BT-20 and BT-474 cells were cultured to subconfluence. On day 0,

medium was exchanged to include DIM at the final concentration of 0 (DMSO control), 50 and 100 μmol/L for BT-20, or 0 (DMSO control), 25, and 50 μmol/L for BT-474. Total cell extract was harvested 24, 48, and 72 h later and probed and analyzed as above.

Real-time Reverse Transcription-PCR Analysis of $p27^{kip}$ Expression after DIM Treatment

BT-20 or BT-474 cells were plated overnight and treated with DIM at the indicated concentrations and harvested 6 and 24 h after exposure. Total RNA was harvested with Trizol (Invitrogen). Total RNA (1 μg) was processed for first-strand cDNA synthesis using TaqMan reverse transcription (RT) reagents kit (Applied Biosystems) in a total volume of 50 μL, including 6.25 units MultiScribe reverse transcriptase and 25 pmol random hexamers. The RT reaction was done at 25°C for 10 min followed by 48°C for 30 min and 95°C for 5 min. The primers used in the PCR were the $p27^{kip}$ and glyceraldehyde-3-phosphate dehydrogenase sequences validated previously by Yakes et al. (20). The primers were checked by verifying the expected product size in a virtual PCR analysis and primer concentration was optimized to avoid primer dimer formation. Also, dissociation curves were checked to confirm specific amplification. Triplicate real-time PCR amplications for each primer set were undertaken in a MX4000 Multiplex QPCR System (Stratagene) using 2× SYBR Green PCR Master Mix (Applied Biosystems). One microliter of the RT reaction was used in a total volume of 25 μL PCR mix. The thermal profile for PCR was 95°C × 10 min followed by 40 cycles of 94°C × 15 s and then 60°C × 1 min. The threshold cycle of each amplification was determined and used to calculate the quantity of RNA based on a serially diluted standard curve of the time 0 control sample. The $p27^{kip}$ product was adjusted to that of general transcription by dividing the quantity of $p27^{kip}$ RNA by that of glyceraldehyde-3-phosphate dehydrogenase for each sample. Finally, the relative $p27^{kip}$ product of each sample was normalized by dividing by the relative $p27^{kip}$ product at time 0 (control). The entire experiment was repeated and relative $p27^{kip}$ signals were plotted as a bar graph showing the means and SDs.

Protein Half-life

BT-20 or BT-474 cells were plated at 1.0×10^6 per 60-mm dishes and cultured overnight. DMSO (control) or DIM was added at a final concentration of 100 μmol/L (BT-20) or 50 μmol/L (BT-474), and the cells were cultured for 24 h. A set of control plates was harvested just before DMSO or DIM was added to study plates. Twenty-four hours after DIM exposure, 25 μg/mL cyclohexamide (C-7698; Sigma) was added, and plates were harvested at 0, 1, 2, 4, 6, 8, 12, 24, and 30 h afterward. Total cell extract was harvested and probed by immunoblotting for $p27^{kip}$ or actin as above. Densitometry of film acquired images was done and normalized to expression at time 0 h after cyclohexamide addition. Half-life was calculated based on appropriate curve fitting algorithms in Prism.

Immunofluorescence Confocal Microscopy

BT-20 or BT-474 cells were cultured overnight on coverslips in six-well dishes at 1.5×10^5 cells per well. The next day, medium was replaced with DIM at 50 μmol/L for BT-474 and 100 μmol/L BT-20 cells, and cells were cultured for 48 h. Cells were fixed with 10% formalin for 10 min, washed with PBS, air dried, and stored at 4°C for less than 1 week. After a PBS wash, coverslips were treated with 0.5% Triton X-100 in PBS for 10 min then incubated at 37°C for 2.5 h with anti-$p27^{kip}$ antibody at 1 μg/mL (K25020; BD Transduction Labs) or control murine IgG at 0.5 μg/mL (12-371; Upstate Biotechnology) in PBS with 0.05% Triton X-100. After three washes in the same buffer, incubation was done with FITC-conjugated anti-mouse antibody at 1:100 (A11029; Molecular Probes) along with 0.1 μg/mL 4′,6-diamidine-2′-phenylindole (Sigma) in the same buffer for 1 h at 37°C. After three washes and air drying, coverslips were mounted with Antifade (Molecular Probes). Images were captured on a Zeiss 310 laser scanning inverted confocal microscope system, using a 63 × 1.2 objective, and 488 and 364 nm laser wavelengths to detect the FITC and 4′,6-diamidine-2′-phenylindole stains, respectively. Images were converted to Adobe Photoshop files and then formatted into PowerPoint images.

Cytoplasmic-Nuclear Fractionation of Cells

BT-474 or BT-20 cells were plated at 6×10^6 per 150-mm dish and cultured until 50% to 60% confluent. Then, DIM was added to a final concentration of 0, 25, or 50 μmol/L. Cells were harvested after 48 or 72 h. Both floating cells and trypsinized cells were collected, washed twice in PBS with trypsin inhibitor (Calbiochem), counted, and pelleted. The pellets were gently resuspended in 2 volumes of sucrose lysis buffer (SL) [0.2 mol/L sucrose, 19 mmol/L Tris-HCl (pH 7.8), 3 mmol/L $CaCl_2$, 2 mmol/L $MgCl_2$, 0.1 mmol/L EDTA, 1 mmol/L DTT, 0.5 mmol/L phenylmethylsulfonyl fluoride, 20 μg/mL aprotinin, 20 μg/mL leupeptin, 20 μg/mL pepstatin] with 0.25% NP-40, and incubated for 30 to 40 min on ice, until lysis of the cytoplasmic membrane to at least 95% was confirmed by trypan staining. Nuclei were pelleted by spinning at 600 × *g* for 6 min at 4°C. Supernatant was removed and saved at -80°C as the cytoplasmic fraction. Nuclei were pelleted again to remove contaminating cytoplasmic debris. The nuclear pellet was gently resuspended and washed twice with 500 μL SL buffer without NP-40 (SL minus NP). The nuclei were gently resuspended in 500 μL SL minus NP buffer then syringed gently through a 21-gauge needle three times. Nuclei were pelleted again, resuspended in SL minus NP buffer, and layered onto a 0.85 mol/L sucrose cushion buffer and centrifuged at 16,000 × *g* for 15 min at 4°C. The pelleted nuclei were washed again with SL minus NP buffer then extracted in high-salt buffer and pelleted (21). This supernatant (nuclear extract) was saved and stored at -80°C. Protein concentration of cytoplasmic and nuclear fractions was measured as above, and 50 μg of each sample were analyzed by immunoblotting. Primary antibodies used were anti-$p27^{kip}$ at 1:1,000 (SC-528; Santa Cruz), anti-MEK at 1:400 (SC-219; Santa Cruz), and anti-retinoblastoma

protein at 1:200 (14001A; PharMingen) proteins. Images were formatted and densitometry was done as other immunoblots. The relative expression of nuclear and cytoplasmic p27^{kip} was expressed by dividing the nuclear or cytoplasmic signals by either retinoblastoma or MEK band signals, respectively, and the relative ratio of nuclear to cytoplasmic expression calculated and bar graphed.

Immunoprecipitation of p27^{kip} in BT-20 Cells

Cells were seeded at 2×10^6 on 100-mm dishes and cultured for 48 h. DIM was added at 0, 50, and 100 μmol/L and incubated for 24 h. Floating and adherent cells were harvested and washed twice with cold PBS. Cells were solubilized with 250 μL lysis buffer [200 mmol/L NaCl, 20 mmol/L Tris-HCl (pH 7.5), 0.5% NP-40, 10% glycerol, 1 mmol/L EDTA, 1.5 mmol/L $MgCl_2$, 50 mmol/L NaF, 1 mmol/L sodium vanadate, 12 mmol/L β-glycerophosphate, 20 mmol/L sodium pyrophosphate, 4% (v/v) protease inhibitor cocktail (Roche), 1 μg/mL pepstatin, 1 mmol/L phenylmethylsulfonyl fluoride, and 1 mmol/L DTT]. After 30 min on ice, samples were pelleted, the supernatants were collected, and protein concentrations were determined. Lysates were precleared by incubating 400 μg lysate with 30 μL Protein G-Plus agarose (Santa Cruz) for 30 min followed by centrifugation. Anti-p27^{kip} antibody (2 μg; Santa Cruz) was added and incubated for overnight at 4°C followed by the addition of 5 μL Protein G-Plus agarose and overnight incubation. After washing four times with 1 mL wash buffer [137 mmol/L NaCl, 20 mmol/L Tris-HCl (pH 7.5), 0.5% NP-40, 10% glycerol, 1 mmol/L EDTA, 1.5 mmol/L $MgCl_2$, and 0.1% Tween 20, 4% (v/v) protease inhibitor cocktail, 1 μg/mL pepstatin, and 1 mmol/L phenylmethylsulfonyl fluoride], pellets were resuspended into immunoblot sample load buffer. SDS-PAGE and immunoblotting were done as described above. Primary antibodies used were anti-p27^{kip} at 1 μg/mL (K25020; BD Transduction Labs), anti-phospho-Thr^{187} residue of p27^{kip} at 1:500 (71-7700; Zymed), and anti-14-3-3 at 1:200 (H-8; Santa Cruz). Immunoblots were developed with appropriate secondary antibodies. Relevant bands were imaged on film and analyzed by densitometry. To determine the relative amount of phospho-p27^{kip} or p27^{kip} associated with 14-3-3, the signals from relevant phospho-Thr^{187} or 14-3-3 bands were divided by the total p27^{kip} detected.

Results

Constitutive Expression of Her-2 and Akt in Breast Cell Lines

The baseline expression of Her-2 was determined in a panel of human breast cancer cell lines that included BT-20, BT-474, MCF-7, and T47D. The assays included the expression of Her-2 activated downstream signaling proteins (phospho-Akt) and p27 proteins that are transcriptionally regulated by Akt. All four cell lines expressed high levels of Akt, but only BT-20 expressed high level of phospho-Akt (Fig. 1A). BT-474 and T47D expressed high and modest levels of Her-2, respectively. However, MCF-7 and BT-20 showed low level of Her-2 (Fig. 1A). The results showed that the Her-2, Akt, and p27 were frequently but differentially dysregulated in the different human breast cancer cell lines.

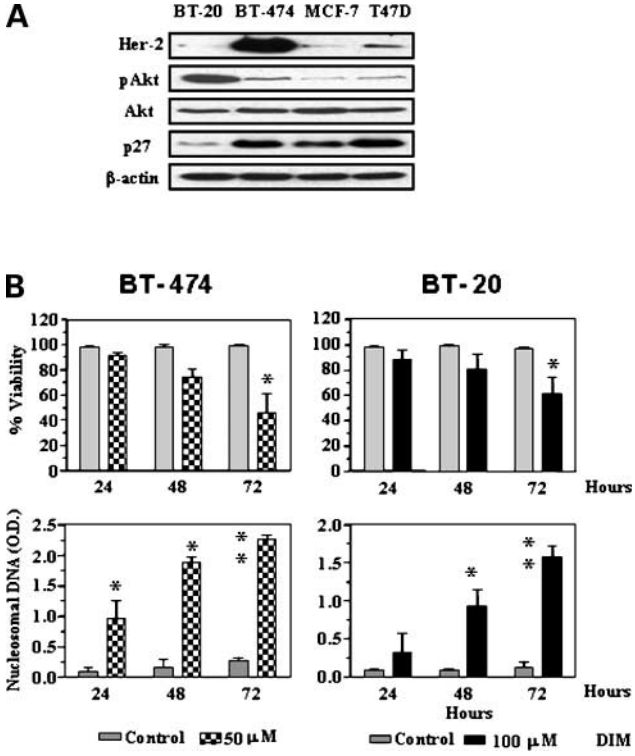

Figure 1. **A,** expression of Her-2, Akt1, phospho-Akt, and p27^{kip} in four human breast cancer cell lines by immunoblot. **B,** DIM induces cell death and apoptosis in BT-474 and BT-20 cells. Mean ± SD ($n = 6$) of three independent experiments. *, $P < 0.05$; **, $P < 0.01$, compared with the control. *Top,* BT-474 cells treated with 50 μmol/L DIM showing effect on cell viability by trypan staining (*top*) and apoptosis as indicated by nucleosomal DNA release (*bottom*). *Bottom,* BT-20 cells treated with 100 μmol/L DIM showing effect on viability (*top*) and apoptosis (*bottom*).

DIM Inhibits Growth and Induces Apoptosis in Multiple Breast Cancer Cell Lines

The effect of DIM on cell growth of breast cancer cells is depicted in Table 1. We found that the IC_{50} after 4 days of DIM exposure for all the cell lines appears to be in a similar range of 30 to 60 μmol/L regardless of Her-2, Akt, or ER status. Because DIM has been reported to modulate Akt, and in view of the observed increased activation of Akt in BT-20 and BT-474 cells, we sought to further define the effects of DIM in these cells. This inhibition of cell proliferation could be due to cell cycle arrest, resulting in the inhibition of cell growth. Alternatively, the inhibition of cell growth could be attributed to the induction of apoptotic cell death induced by DIM in breast cancer cells. Therefore, we investigated whether DIM could induce apoptosis in these cells. The effects of DIM on apoptosis are shown in Fig. 1B. In BT-474 cells, the induction of apoptosis occurred at 24 h and the decrease in viability by 48 h, whereas the same events occurred about 24 h later, respectively, in BT-20 cells.

Table 1. Breast cancer cell line characteristics and sensitivity to DIM

Cell line	Relative expression		Functional ER-α	DIM IC_{50} (μmol/L), mean ± SD
	Her-2	Phospho-Akt		
BT-20	Low	High	–	56 ± 9
BT-474	High	Modest	+	25 ± 6
T47D	Low	Low	+	34 ± 1
MCF-7	Low	Low	+	50 ± 8

Effect of DIM on Akt and p27^{kip} over Time in BT-20 and BT-474 Cell Lines

Because others have reported that I3C induces p21 and p27^{kip} in MCF-7 cells after about 60 h of exposure (11), we studied the time course of effects in both cell lines. As seen in Fig. 2A, the induction of p27^{kip} by DIM began at 24 h in both BT-20 and BT-474 cell lines. In BT-20 cells, inhibition of expression of activated and phospho-Akt also occurred but only at 48 h. The results of multiple independent experiments in BT-20 cells show that induction of p27^{kip} expression occurred before decreased Akt activation (Fig. 2B). Moreover, this induction of p27^{kip} appeared to occur at or before significant loss of cell viability or apoptosis (Fig. 1B). Thus, p27^{kip} induction preceded these events. DIM at 25 or 50 μmol/L did not inhibit Akt expression or activation in BT-474 cells (data not shown).

DIM Induces p27^{kip} Expression by Both Transcription and Prolonging Protein Half-life

In both BT-474 and BT-20 cells, DIM induced p27^{kip} transcript expression as measured by real-time RT-PCR (Fig. 3A). This occurred as early as 6 h after DIM exposure, at 50 and 100 μmol/L, respectively. Because ubiquitination-dependent degradation of p27^{kip} is dependent on phosphorylation of p27^{kip} by cyclin-dependent kinases (cdk; ref. 22), and because I3C is known to inhibit cdk6 (11), we studied if DIM prolonged the half-life of p27^{kip} protein. As shown in Fig. 3B, BT-20 cells exposed to 100 μmol/L DIM for 24 h significantly prolong p27^{kip} half-life from 3.9 to 27 h. However, in BT-474 cells, 50 μmol/L DIM did not prolong the half-life compared with control DMSO, with half-lives of 8.8 and 8.5 h, respectively (data not shown), indicating that this effect is not universal.

DIM Induces Nuclear Translocation of p27^{kip}

Recent work by others has shown that p27^{kip} expression and localization may also be modulated by its phosphorylation by several serine-threonine kinases, including Akt and cdk2 (18). Confocal experiments showed that DIM at 50 μmol/L treatment for 48 h significantly induced nuclear expression of p27^{kip} in BT-474 cells (Fig. 4A). A similar increase in nuclear p27^{kip} was also detected by confocal microscopy in the nuclei of BT-20 cells exposed to 100 μmol/L DIM (data not shown). This was confirmed by cell fractionation studies in the BT-474 cells (Fig. 4B) and BT-20 cells (data not shown). These results clearly provided evidence in support of our conclusion showing a dose- and time-dependent increase in nuclear expression of p27^{kip} by DIM treatment.

DIM Induces a Relative Decrease in p27^{kip} Phosphorylation at Thr^{187} and Its Association with 14-3-3 in BT-20 Cells

Immunoprecipitation experiments confirmed the induction of p27^{kip} and also indicated that DIM can induce changes in the molecular status of p27^{kip}. BT-20 cells treated with DIM for 24 h resulted in a relative dose-dependent decrease in phosphorylation at residue Thr^{187} of p27^{kip} (Fig. 5B). This change in p27^{kip} status is consistent with a mechanism in which DIM inhibits cdk-dependent

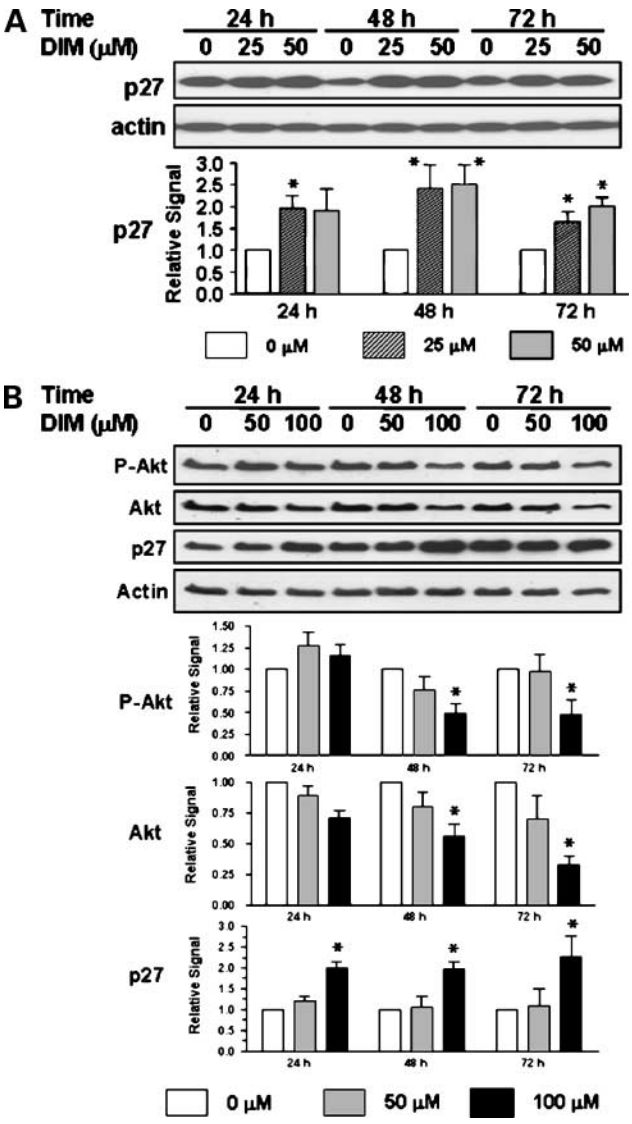

Figure 2. DIM induces p27^{kip} in breast cancer cells. **A,** DIM induces p27^{kip} in BT-474 cells. **B,** DIM induces p27^{kip} while inhibiting Akt and phospho-Akt expression in BT-20 cells. Immunoblots are representative of at least three blots from two or more independent experiments. The bar graphs are based on densitometric values of bands of interest normalized to actin from at least three immunoblots from two independent experiments. *Bars,* SD. *, $P < 0.05$, compared with the control.

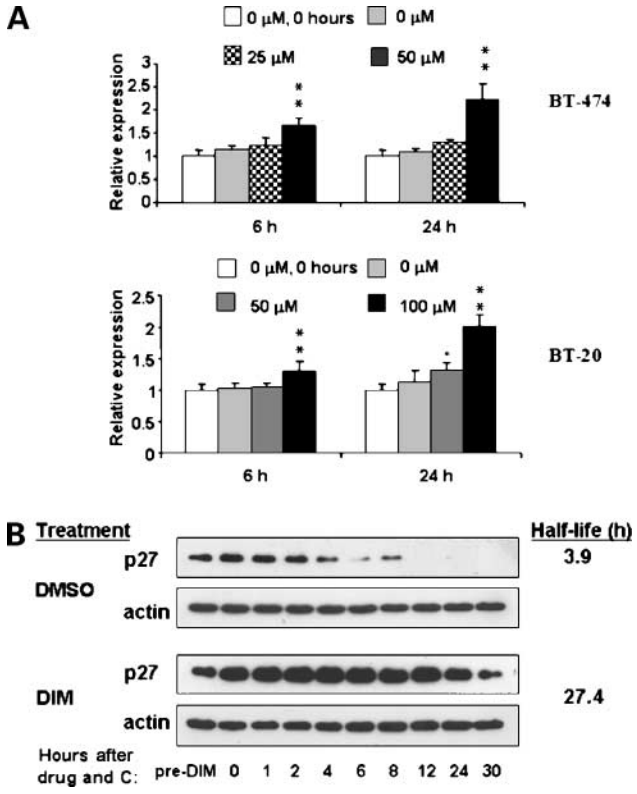

Figure 3. **A,** DIM induces p27^{kip} transcript expression as early as 6 h after exposure by real-time RT-PCR analysis. *Top,* BT-474 cells after 50 μmol/L DIM treatment; *bottom,* BT-20 cells after 100 μmol/L DIM treatment. Results are normalized to actin expression and represent the mean ± SD from a total of three RT-PCR runs from RNA harvested from two independent experiments. *, $P < 0.05$; **, $P < 0.01$, compared with the control. **B,** DIM induces significant increase in p27^{kip} protein half-life in BT-20 cells. Extracts were harvested before addition of DIM (''pre-DIM''), or after 24 h, when DMSO or 100 μmol/L DIM and cycloheximide (**C**) were added.

phosphorylation of this site, therefore restricting ubiquitin-dependent proteolysis, and promoting prolongation of its protein half-life. In addition, probing for the 14-3-3 protein showed that there was a relative decrease in the amount of p27^{kip} associated with 14-3-3 (Fig. 5B). Because 14-3-3 can sequester p27^{kip} to the cytoplasm, one mechanism of its nuclear localization may be the loss of association with 14-3-3.

Discussion

In this report, we show in human breast cancer cells that DIM induces p27^{kip} before the induction of apoptosis and cell death. Therefore, the modulation of p27^{kip} may play a role in its mechanisms of action. We show that the induction of p27^{kip} may occur by increasing transcription in both BT-20 and BT-474 cell lines and by the prolongation of p27^{kip} half-life in BT-20 cells. Moreover, we show, for the first time, that DIM induces nuclear localization of p27^{kip}, an event that is relevant to its primary function in inhibiting cdks and inducing growth arrest. The induction of p27^{kip} may also directly trigger apoptosis in human breast cancer cell lines and other cell lines, independent of the inhibition of Akt signaling, as evidenced by results from p27^{kip} gene transfer studies (23, 24).

The mechanisms of modulation of p27^{kip} are relatively complex, occurring at transcriptional, translational, and post-translational levels. Therefore, we explored potential mechanisms. First, we show that DIM induces its transcription as early as 6 h after exposure (Fig. 3A). Because Akt activation is inhibited by DIM, the induction of p27^{kip} is consistent with a model in which DIM reverses the Akt-dependent repression of the forkhead family of transcription factors (14, 25). These activated transcription factors are known to specifically transactivate the p27^{kip} promoter (15). Ectopic expression of forkhead-type transcription factors in a variety of cell lines, including human colon carcinoma cells, has been shown to consistently trigger p27^{kip} expression and cell cycle arrest (26). Moreover, the effects of DIM are consistent with those of inhibitors of phosphatidylinositol-3-kinase, such as LY294002 and Wortmannin, which have been shown to inhibit Akt activation, activate the forkhead member, AFX, and induce expression of p27^{kip} (27).

DIM may activate the p27^{kip} promoter through other control elements in its structure, such as those that bind Sp1, nuclear factor-κB, CRE, and Myb related elements (28). Sp1 may be involved, because I3C can inhibit cdk6 promoter activity, and this is dependent on a Sp1-binding site in MCF-7 breast cancer cells (29). Modulation of nuclear factor-κB may also be relevant, because DIM can inhibit nuclear factor-κB activation in breast cancer cells (12). Because the induction of p27^{kip} transcription and expression appears to precede inhibition of Akt in BT-20 cells, and inhibition of Akt was not observed in BT-474 cells, transcription factors other than the forkhead family are likely to be involved.

Other important mechanisms of p27^{kip} induction by DIM described in this report are related to its post-translational processing. For example, DIM significantly prolonged its protein half-life in BT-20 cells. Because it has been shown that p27^{kip} has several sites of phosphorylation that control its proteolytic fate, we examined the status of phosphorylation at Thr^{187}, which when phosphorylated facilitates the binding of the ubiquitin-ligase complex, ubiquitination, and proteolysis (18). DIM treatment caused a relative decrease in phospho-Thr^{187} in BT-20 cells as early as 24 h (Fig. 5), in the same timeframe as the observed prolongation of p27^{kip} half-life. Therefore, our data support a mechanism in BT-20 cells that operates through blockade of Thr^{187} phosphorylation, thus preventing its ubiquitination and degradation. The exact kinase responsible for phosphorylation at this site targeted by DIM remains to be clarified. Because Fujita et al. reported that Akt can phosphorylate this site (17), our observation on the induction of p27^{kip} protein expression at approximately the same time as a decrease in Akt protein expression (Fig. 2B) supports a mechanism in which DIM inhibits Akt-dependent phosphorylation of p27^{kip}. Targeting of

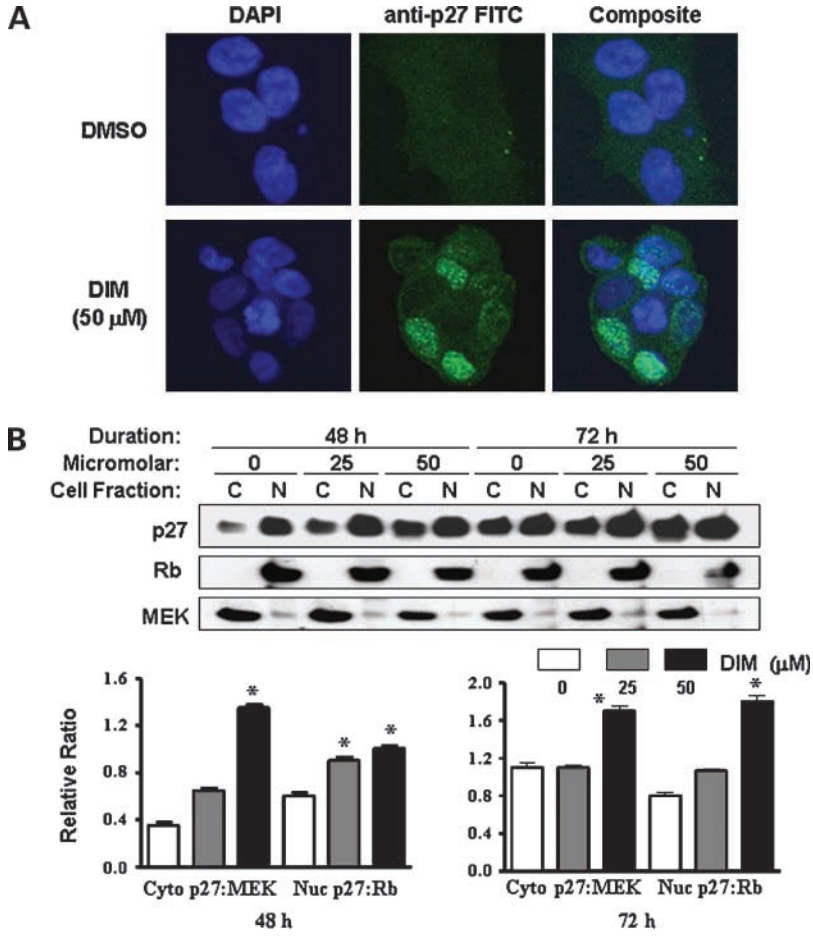

Figure 4. **A,** DIM at 50 μmol/L induces nuclear localization of $p27^{kip}$ in BT-474 cells by confocal microscopy after 48 h of exposure. **B,** DIM induces cytoplasmic and nuclear $p27^{kip}$ expression by cell fractionation analysis in BT-474 cells. *Top,* immunoblot showing $p27^{kip}$ induction in both cytoplasmic and nuclear fractions and verification of cell fractionation by MEK and retinoblastoma immunoblots; *bottom,* $P27^{kip}$ induced in both fractions, but overall higher levels in nucleus, as confirmed by densitometric comparison of induction of cytoplasmic or nuclear $p27^{kip}$, normalized to respective MEK or retinoblastoma expression (*bottom*). *, $P < 0.05$, compared with the control.

cdk2 or cdk6 is also possible, because cdk2 and cdk6 are known to phosphorylate Thr^{187} (17, 30), and Cover et al. has found that I3C can inhibit cdk6 expression and activity in breast cancer cells (11). Although mitogen-activated protein kinase has also been reported to phosphorylate Thr^{187} (31), we observed that DIM does not alter expression of phospho-Erk, suggesting that DIM does not inhibit the mitogen-activated protein kinase pathway (data not shown). For BT-474 cells, prolongation of protein half-life was not found, suggesting other mechanisms of induction. This is consistent with the observed lack of inhibition of Akt activation in BT-474 cells at the doses tested.

We also show for the first time that DIM induces nuclear localization of $p27^{kip}$ in human breast cancer cells. This is shown by both confocal microscopy and cell fractionation experiments in both BT-474 and BT-20 cells (Fig. 4). This is

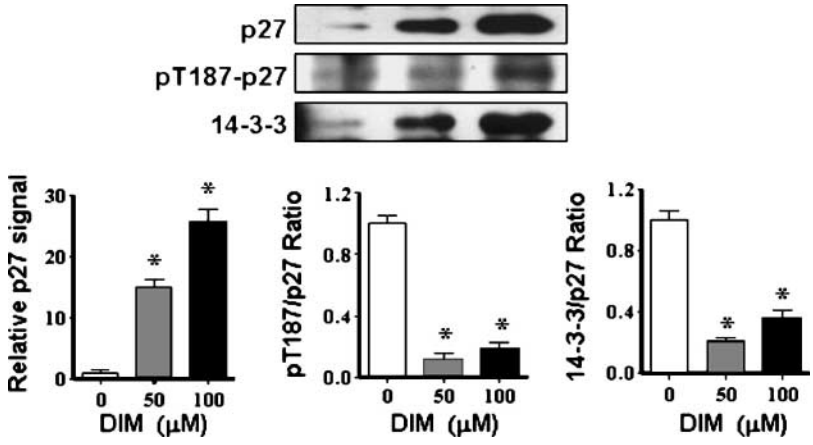

Figure 5. Molecular status of induced $p27^{kip}$ is in BT-20 cells after exposure to DIM for 24 h. BT-20 cells were exposed to DIM at the indicated concentrations followed by immunoprecipitation of $p27^{kip}$ from cell extracts. *Top,* immunoblots for $p27^{kip}$, phospho-Thr^{187}-$p27^{kip}$ (*pT187-p27*), and the 14-3-3 protein; *bottom,* densitometry analysis of immunoblots indicates induction of $p27^{kip}$ (*left*), a relative decrease in the fraction of $p27^{kip}$ that is phosphorylated at Thr^{187} (*middle*), and relative decrease in the amount of 14-3-3 associated with $p27^{kip}$ (*right*). *, $P < 0.01$, compared with the control.

functionally relevant as cyclin A/E-cdk2 complexes are optimally accessible to p27^{kip} binding and inhibition in the nucleus. This is also consistent with the observation that in primary breast cancer tissues p27^{kip} is frequently abnormally localized to the cytoplasm (32). Therefore, DIM may inhibit breast cancer growth by inducing nuclear localization of p27^{kip}, which then initiates G_0-G_1 cell cycle arrest, consistent with the effects of I3C (11, 33). Once again, there may be multiple mechanisms for changes in p27^{kip} cellular distribution. For example, Fujita et al. have shown explicitly that Akt can phosphorylate the Thr^{198} residue of p27^{kip} and that this site (and not Ser^{10} or Thr^{187}) is responsible for 14-3-3 binding and secondary cytoplasmic localization (17). Our data show that DIM causes a relative decrease in 14-3-3 associated with p27^{kip} (Fig. 5), consistent with the increase in nuclear localization observed. Akt-dependent phosphorylation of Thr^{157} is another mechanism that impairs nuclear import of p27^{kip} and G_0-G_1 arrest in human breast cancer cells and tumors (32, 34). Indirect modulation of this phosphorylation site by DIM may also contribute to nuclear localization. It is important to mention that DIM induced p27 expression, which could be dependent on cell type. It has been reported that DIM do not induce p27 expression in MDA-MB-231 and MCF-7 breast cancer cell lines (10, 35). Our microarray data also showed that p27 expression was not changed in MDA-MB-231 breast cancer cells treated with DIM.[3] Moreover, we found that DIM also did not induce p27 expression in MCF10CA1a breast cancer cell lines (data not shown).

The findings that DIM inhibits Akt and induces p27^{kip} in breast cancer cells should stimulate further investigation, because human breast cancers often overexpress activated Akt (36), underexpress p27^{kip} (37), or have cytoplasmic localization of p27^{kip} (32). The underexpression of p27^{kip} is associated with advance stage and appears to be an important independent negative survival factor (37, 38). Both Akt inhibition and the induction of p27^{kip} may independently contribute to stimulating apoptosis in breast cancer cells (39, 40). The effects of DIM occur even in Her-2- or Akt-overexpressing breast cancer cells, such as BT-20 and BT-474. Inducing p27^{kip} may be a particularly relevant effect of DIM in Her-2-overexpressing cells based on our results, because Her-2 has been shown to repress p27^{kip} expression and nuclear localization (19, 20), and inhibition of Her-2 signaling induces p27^{kip} (20, 21). It is possible that DIM may also inhibit signaling at levels upstream to Akt, such as at the Her-2 receptor, because we have reported previously that I3C can repress epidermal growth factor receptor expression and activation in prostate cancer cells (41).

In summary, our data showed that DIM can inhibit growth and survival of breast cancer cells in spite of Her-2 or Akt overexpression or in the absence of ER. Furthermore, we propose a model in which DIM induces apoptosis and cell cycle arrest by several mechanisms, including the inhibition of Akt, induction of p27^{kip} expression, and nuclear localization of p27^{kip}. Additional *in vitro* and *in vivo* studies are needed to further define the mechanisms of action and to assess the potential role of DIM in the prevention of human breast cancer.

[3] Unpublished data.

References

1. Jemal A, Siegel R, Ward E, Murray T, Xu J, Thun MJ. Cancer statistics, 2007. CA Cancer J Clin 2007;57:43 – 66.
2. Jordan VC. Chemoprevention of breast cancer with selective oestrogen-receptor modulators. Nat Rev Cancer 2007;7:46 – 53.
3. Thuerlimann B, Koeberle D, Senn HJ. Guidelines for the adjuvant treatment of postmenopausal women with endocrine-responsive breast cancer: past, present and future recommendations. Eur J Cancer 2007;43:46 – 52.
4. Davis DL, Telang NT, Osborne MP, Bradlow HL. Medical hypothesis: bifunctional genetic-hormonal pathways to breast cancer. Environ Health Perspect 1997;105 Suppl 3:571 – 6.
5. Grubbs CJ, Steele VE, Casebolt T, et al. Chemoprevention of chemically-induced mammary carcinogenesis by indole-3-carbinol. Anticancer Res 1995;15:709 – 16.
6. Malloy VL, Bradlow HL, Orentreich N. Interaction between a semisynthetic diet and indole-3-carbinol on mammary tumor incidence in Balb/cfC3H mice. Anticancer Res 1997;17:4333 – 7.
7. Dashwood RH, Fong AT, Arbogast DN, Bjeldanes LF, Hendricks JD, Bailey GS. Anticarcinogenic activity of indole-3-carbinol acid products: ultrasensitive bioassay by trout embryo microinjection. Cancer Res 1994;54:3617 – 9.
8. Chen I, McDougal A, Wang F, Safe S. Aryl hydrocarbon receptor-mediated antiestrogenic and antitumorigenic activity of diindolylmethane. Carcinogenesis 1998;19:1631 – 9.
9. Ge X, Fares FA, Yannai S. Induction of apoptosis in MCF-7 cells by indole-3-carbinol is independent of p53 and bax. Anticancer Res 1999;19:3199 – 203.
10. Vanderlaag K, Samudio I, Burghardt R, Barhoumi R, Safe S. Inhibition of breast cancer cell growth and induction of cell death by 1,1-bis(3′-indolyl)methane (DIM) and 5,5′-dibromoDIM. Cancer Lett 2006;236:198 – 212.
11. Cover CM, Hsieh SJ, Tran SH, et al. Indole-3-carbinol inhibits the expression of cyclin-dependent kinase-6 and induces a G_1 cell cycle arrest of human breast cancer cells independent of estrogen receptor signaling. J Biol Chem 1998;273:3838 – 47.
12. Rahman KW, Sarkar FH. Inhibition of nuclear translocation of nuclear factor-κB contributes to 3,3′-diindolylmethane-induced apoptosis in breast cancer cells. Cancer Res 2005;65:364 – 71.
13. Toker A, Yoeli-Lerner M. Akt signaling and cancer: surviving but not moving on. Cancer Res 2006;66:3963 – 6.
14. Rena G, Guo S, Cichy SC, Unterman TG, Cohen P. Phosphorylation of the transcription factor forkhead family member FKHR by protein kinase B. J Biol Chem 1999;274:17179 – 83.
15. Dijkers PF, Medema RH, Pals C, et al. Forkhead transcription factor FKHR-L1 modulates cytokine-dependent transcriptional regulation of p27(KIP1). Mol Cell Biol 2000;20:9138 – 48.
16. Liang J, Zubovitz J, Petrocelli T, et al. PKB/Akt phosphorylates p27, impairs nuclear import of p27 and opposes p27-mediated G1 arrest. Nat Med 2002;8:1153 – 60.
17. Fujita N, Sato S, Katayama K, Tsuruo T. Akt-dependent phosphorylation of p27Kip1 promotes binding to 14-3-3 and cytoplasmic localization. J Biol Chem 2002;277:28706 – 13.
18. Vlach J, Hennecke S, Amati B. Phosphorylation-dependent degradation of the cyclin-dependent kinase inhibitor p27. EMBO J 1997;16:5334 – 44.
19. Yang HY, Zhou BP, Hung MC, Lee MH. Oncogenic signals of HER-2/neu in regulating the stability of the cyclin-dependent kinase inhibitor p27. J Biol Chem 2000;275:24735 – 9.
20. Yakes FM, Chinratanalab W, Ritter CA, King W, Seelig S, Arteaga CL. Herceptin-induced inhibition of phosphatidylinositol-3 kinase and Akt Is

required for antibody-mediated effects on p27, cyclin D1, and antitumor action. Cancer Res 2002;62:4132 – 41.

21. Lane HA, Motoyama AB, Beuvink I, Hynes NE. Modulation of p27/Cdk2 complex formation through 4D5-mediated inhibition of HER2 receptor signaling. Ann Oncol 2001;12 Suppl 1:S21 – 22.

22. Carrano AC, Eytan E, Hershko A, Pagano M. SKP2 is required for ubiquitin-mediated degradation of the CDK inhibitor p27. Nat Cell Biol 1999;1:193 – 9.

23. Craig C, Wersto R, Kim M, et al. A recombinant adenovirus expressing p27Kip1 induces cell cycle arrest and loss of cyclin-Cdk activity in human breast cancer cells. Oncogene 1997;14:2283 – 9.

24. Katayose Y, Kim M, Rakkar AN, Li Z, Cowan KH, Seth P. Promoting apoptosis: a novel activity associated with the cyclin-dependent kinase inhibitor p27. Cancer Res 1997;57:5441 – 5.

25. Brunet A, Bonni A, Zigmond MJ, et al. Akt promotes cell survival by phosphorylating and inhibiting a Forkhead transcription factor. Cell 1999; 96:857 – 68.

26. Kops GJ, Medema RH, Glassford J, et al. Control of cell cycle exit and entry by protein kinase B-regulated forkhead transcription factors. Mol Cell Biol 2002;22:2025 – 36.

27. Collado M, Medema RH, Garcia-Cao I, et al. Inhibition of the phosphoinositide 3-kinase pathway induces a senescence-like arrest mediated by p27Kip1. J Biol Chem 2000;275:21960 – 8.

28. Philipp-Staheli J, Payne SR, Kemp CJ. p27(Kip1): regulation and function of a haploinsufficient tumor suppressor and its misregulation in cancer. Exp Cell Res 2001;264:148 – 68.

29. Cram EJ, Liu BD, Bjeldanes LF, Firestone GL. Indole-3-carbinol inhibits CDK6 expression in human MCF-7 breast cancer cells by disrupting Sp1 transcription factor interactions with a composite element in the CDK6 gene promoter. J Biol Chem 2001;276:22332 – 40.

30. Ellis M, Chew YP, Fallis L, et al. Degradation of p27(Kip) cdk inhibitor triggered by Kaposi's sarcoma virus cyclin-cdk6 complex. EMBO J 1999; 18:644 – 53.

31. Lenferink AE, Simpson JF, Shawver LK, Coffey RJ, Forbes JT, Arteaga CL. Blockade of the epidermal growth factor receptor tyrosine kinase suppresses tumorigenesis in MMTV/Neu + MMTV/TGF-alpha bigenic mice. Proc Natl Acad Sci U S A 2000;97:9609 – 14.

32. Viglietto G, Motti ML, Bruni P, et al. Cytoplasmic relocalization and inhibition of the cyclin-dependent kinase inhibitor p27(Kip1) by PKB/Akt-mediated phosphorylation in breast cancer. Nat Med 2002;8: 1136 – 44.

33. Cover CM, Hsieh SJ, Cram EJ, et al. Indole-3-carbinol and tamoxifen cooperate to arrest the cell cycle of MCF-7 human breast cancer cells. Cancer Res 1999;59:1244 – 51.

34. Shin I, Yakes FM, Rojo F, et al. PKB/Akt mediates cell-cycle progression by phosphorylation of p27(Kip1) at threonine 157 and modulation of its cellular localization. Nat Med 2002;8:1145 – 52.

35. Hong C, Kim HA, Firestone GL, Bjeldanes LF. 3,3′-Diindolylmethane (DIM) induces a G(1) cell cycle arrest in human breast cancer cells that is accompanied by Sp1-mediated activation of p21(WAF1/CIP1) expression. Carcinogenesis 2002;23:1297 – 305.

36. Nakatani K, Thompson DA, Barthel A, et al. Up-regulation of Akt3 in estrogen receptor-deficient breast cancers and androgen-independent prostate cancer lines. J Biol Chem 1999;274:21528 – 32.

37. Tan P, Cady B, Wanner M, et al. The cell cycle inhibitor p27 is an independent prognostic marker in small (T1a,b) invasive breast carcinomas. Cancer Res 1997;57:1259 – 63.

38. Fredersdorf S, Burns J, Milne AM, et al. High level expression of p27(kip1) and cyclin D1 in some human breast cancer cells: inverse correlation between the expression of p27(kip1) and degree of malignancy in human breast and colorectal cancers. Proc Natl Acad Sci U S A 1997; 94:6380 – 5.

39. Downward J. Mechanisms and consequences of activation of protein kinase B/Akt. Curr Opin Cell Biol 1998;10:262 – 7.

40. Sgambato A, Cittadini A, Faraglia B, Weinstein IB. Multiple functions of p27(Kip1) and its alterations in tumor cells: a review. J Cell Physiol 2000;183:18 – 27.

41. Chinni SR, Sarkar FH. Akt inactivation is a key event in indole-3-carbinol-induced apoptosis in PC-3 cells. Clin Cancer Res 2002;8: 1228 – 36.